Original Investigation

Kidney360

Lrpap1 (RAP) Inhibits Proximal Tubule Clathrin Mediated and Clathrin Independent Endocytosis, Ameliorating Renal Aminoglycoside Nephrotoxicity

Mark C. Wagner, Ruben M. Sandoval, Shiv Pratap S. Yadav, Silvia B. Campos, George J. Rhodes, Carrie L. Phillips, and Bruce A. Molitoris

Key Points

- Proximal tubule endocytosis of toxins often leads to nephrotoxicity.
- Inhibition of endocytosis with receptor-associated protein may serve as a clinical approach to reduce or eliminate kidney damage from a potential nephrotoxin.

Abstract

Background Proximal tubules (PTs) are exposed to many exogenous and endogenous nephrotoxins that pass through the glomerular filter. This includes many small molecules, such as aminoglycoside and myeloma light chains. These filtered molecules are rapidly endocytosed by the PTs and lead to nephrotoxicity.

Methods To investigate whether inhibition of PT uptake of filtered toxins can reduce toxicity, we evaluated the ability of Lrpap1 or receptor-associated protein (RAP) to prevent PT endocytosis. Munich Wistar Frömter rats were used since both glomerular filtration and PT uptake can be visualized and quantified. The injury model chosen was the well-established gentamicin-induced toxicity, which leads to significant reductions in GFR and serum creatinine increases. CKD was induced with a right uninephrectomy and left 40-minute pedicle clamp. Rats had 8 weeks to recover and to stabilize GFR and proteinuria. Multiphoton microscopy was used to evaluate endocytosis *in vivo* and serum creatinine, and 24-hour creatinine clearances were used to evaluate kidney functional changes.

Results Studies showed that preadministration of RAP significantly inhibited both albumin and dextran endocytosis in outer cortical PTs. Importantly, this inhibition was found to be rapidly reversible with time. RAP was also found to be an excellent inhibitor of PT gentamicin endocytosis. Finally, gentamicin administration for 6 days resulted in significant elevation of serum creatinine in vehicle-treated rats, but not in those receiving daily infusion of RAP before gentamicin.

Conclusions This study provides a model for the potential use of RAP to prevent, in a reversible manner, PT endocytosis of potential nephrotoxins, thus protecting the kidney from damage.

KIDNEY360 4: 591–605, 2023. doi: https://doi.org/10.34067/KID.0000000000000094

Introduction

Up to 20% of hospitalizations for patients with AKI are due to nephrotoxins.[1] The proximal tubule (PT) is exposed to many exogenous and endogenous potential nephrotoxins filtered across the glomerulus and is in large part responsible for the resulting AKI. This is especially true for molecules with molecular weights <20 kDa that have minimal or no protein binding to plasma components, allowing for their rapid glomerular filtration. PTs have a remarkably rapid, efficient, and effective endocytic uptake rate with S1>S2>>S3.[2] After PT endocytosis, many of these molecules are concentrated within cell lysosomes and other components of the endocytic system. Notable examples include proteins; antibiotics, such as aminoglycosides, myeloma light chains; oligonucleotides; myoglobin; and hemoglobin. This rapid uptake and concentration of filtered molecules, and resulting toxicity, has limited the use of numerous newly developed small molecular weight therapeutics.[3] These include direct cellular toxins, such as radiotherapeutics and other anticancer agents. To avoid this unwanted side effect, creative molecular approaches that enhance noncovalent binding to serum albumin or insert an albumin-binding site

Indiana Center for Biological Microscopy, Indiana University School of Medicine, Indianapolis, Indiana

Correspondence: Dr. Bruce A. Molitoris, 6452 South Himalaya Ctourt, Centennial, CO 80016. Email: bmolitor@iu.edu

into these therapeutic agents are being developed to lengthen drug serum half-life, thus minimizing glomerular filtration and reducing PT exposure and toxicity.

PT endocytosis consists of both clathrin-mediated endocytosis (CME) and clathrin independent endocytosis (CIE), which includes fluid phase endocytosis[2,4–7]. Megalin (LDL receptor-related protein 2) and cubilin (CUBN) are known to be required for PT CME of nearly 100 different molecular species, including potential nephrotoxins.[5] CME is especially prominent in the S1 segment of the PT. The role of CIE of nephrotoxins has received less attention, but is a prominent event in S2 PT cells.[8]

Alpha 2-macroglobulin receptor-associated protein (RAP), Lrpap1 (RAP), was first identified as a 39-kDa protein copurifying with the LDL receptor-related protein (LRP) and was shown to inhibit LRP ligand binding during its biosynthesis.[9] Other studies documented this important role for multiple LDL receptor family members, including megalin.[10] Subsequent studies used RAP to inhibit multiple ligands, such as myeloma light chains,[11] transferrin,[12] and albumin,[13] from binding to megalin or other LDL receptors *in vitro* and albumin *in vivo*.[14] While RAP inhibits multiple ligand LDL receptor interactions, whether it affects indirectly or directly other membrane proteins or trafficking pathways has not been explored. Therefore, the purpose of these studies was to characterize the PT handling of RAP and to determine its effects on PT endocytosis. Interestingly, while the inhibition of CME was expected, the inhibition of CIE was found but not expected. These studies indicate that RAP temporarily blocks PT uptake of both CME and CIE. Furthermore, the data indicate that RAP can have potential therapeutic use as a short-term inhibitor of PT endocytosis of nephrotoxins.

Materials and Methods

Animals

Munich Wistar Frömter (MWF) rats were derived from a colony generously provided by Dr. Roland Blantz (UCSF, San Diego, CA) and maintained in the Indiana University Large Animal Research Center. All experiments followed National Institutes of Health Guidelines for the Care and Use of Laboratory Animals and were approved by the Animal Care and Use Committee at the Indiana University School of Medicine.

RAP and Stable RAP Synthesis, Protein Production, and Purification

Rat RAP had its sequence optimized using Genscript services. The sequence was cloned into the pcDNA3.4 mammalian expression vector that contains the cytomegalovirus promoter, followed by an N-terminus ×6 hisitidine tag. Stable RAP (sRAP) is a form of RAP with increased binding affinity to receptors at low pH, thus lengthening the time in which ligand binding is inhibited and extending its biological half-life of inhibiting endocytosis. sRAP consists of three amino acid changes to RAP as described and characterized by the Strickland laboratory.[15] Our expectation was that sRAP would provide greater megalin-dependent endocytosis inhibition *in vivo* similar to what was shown in its initial *in vitro* and *in vivo* characterization when analyzing α_2-macroglobulin internalization.[15] Expression of each protein took place in the Gibco Expi293F expression system using the Expi293F cells according to the manufacturer's protocol. Purification consisted of affinity binding to Qiagen Ni-NTA superflow nickle-charged resin, followed by a HW55S size exclusion chromatography column. Fractions containing RAP or sRAP, >95% purity, are pooled, concentrated, dialyzed into saline, and lyophilized. Representative examples of both the NiNTA and HW55S columns are shown in Supplemental Figure 1.

Normal and sRAP Dosing

In studies quantifying the effect of PT, endocytosis RAP or sRAP was administered iv (intravenously) at a dose of 40 mg/kg of rat body weight. Administration was done using 0.9% saline as a carrier at a concentration of 20 mg/ml (*i.e.*, a 250-g rat would receive 10 mg in 500 μl). Each figure legend specifies whether RAP or sRAP was used in the study.

Fluorescent Compounds

A 10-kDa cascade blue (CB) anionic dextran (Thermofisher, Waltham, MA) was used as a CIE marker, given iv in 0.9% saline at a dose of 6 mg/kg as previously reported.[16] A Texas Red-X albumin conjugate consisting of seven-atom aminohexanoyl spacer ("X") between the fluorophore and the succinimidyl ester group (Thermofisher, Waltham, MA) and rat serum albumin (RSA) (Sigma Aldrich, St. Louis, MO) was used as a marker for CME uptake. Fluorophore conjugation and dosing have been previously described.[17] The two RAPs were conjugated to Texas Red with a target dye:protein ratio of 1:1. Texas Red gentamicin (TRG) (Biosynthesis, Lewisville, TX, custom synthesis) was given as an iv (intravenous) infusion of 1.0 mg in 500 μl of saline over 30 seconds.

In Vivo RAP Infusion, Uptake, and Effect on Endocytosis

To evaluate cellular uptake and distribution of RAP in the kidney, intravital two-photon studies were undertaken in 8–10-week-old male and female MWF rats that have surface glomeruli.[18] Texas Red conjugated RAP (TR-RAP) was infused, 40 mg/kg iv, followed 10 minutes later by iv infusion of Texas Red-RSA (TR-RSA) to address the effect on CME. RAP's effect on CIE was addressed in a similar manner by infusing RAP, followed by 10-kDa CB dextran (CBdex) (4–6 mg/kg). PT fluorescence accumulation was followed for 60 minutes, and each probe's uptake is reported as fluorescence units/μm^2 and then normalized to the highest value between the vehicle and RAP-treated rat groups in two groups designated S1 (PTs with a clear glomerular opening determined by two-photon microscopy) and PT (consisting of S1 PTs without a clear opening and S2 PT segments). Notably, no S3 PTs extend to the outer cortex accessible to the two-photon imaging performed here, which was limited to approximately 50 μm deep for quantitation.[19,20] In addition, identification of different tubule types is also possible due to the endogenous autofluorescence and apical brush border membrane present in the PTs but lacking from collecting ducts or distal tubules (dt).[20,21] To examine any reduction in the uptake of the markers because of RAP administration, regions containing glomeruli and S1 segments were selected for study and marked, with images obtained at time points of 15, 30, and 60 minutes after bolus infusion of the two markers. Fluorescence from the images was quantified and normalized to the highest average value in the time series.

Evaluation of Aminoglycoside Endocytosis

Quantitative analysis of aminoglycoside endocytosis in PTs after RAP administration was initially studied using TRG in normal MWF rats by monitoring TRG accumulation within the tubular epithelia using multiphoton microscopy. To quantify TRG uptake, images were acquired at approximately 15, 30, and 60-minute intervals after TRG infusion and processed as described for the TR-RSA and CBdex studies. Both RAP and sRAP were evaluated in this time frame to determine any differences in PT gentamicin uptake.

Recovery of Endocytyosis

Because RAP reduced both CME and CIE in PTs, a study was conducted to see whether endocytic function would return. sRAP was infused into MWF rats, as before, followed by a 4-hour recovery and then an iv infusion of TR-RSA and CBdex. The rats were then imaged for 60 minutes, as above, to quantify PT uptake. sRAP was evaluated because of the increased inhibition over RAP observed for fluorescent gentamicin uptake.

Aminoglycoside Studies in Normal and CKD Rats

On the basis of our earlier aminoglycoside nephrotoxicity studies,[22,23] an MWF rat CKD model was used. This consisted of a right unilateral nephrectomy and 40-minute clamp of the left contralateral kidney in twelve 16-week-old male MWF rats, as previously reported.[24] Rats after surgery were allowed to recover for 4 weeks and then were studied for the effects of the nephrectomy and clamp. Their serum creatinine had increased from 0.54±0.05 mg/dl to 0.80±0.23 mg/dl; 24-hour urinary creatinine clearances had decreased from 1.29±0.15 to 0.86±0.27 ml/min, and 24-hour urinary protein had increased from 126.2±56.7 to 211.6±64.6 mg/24 h (all had $P < 0.05$). Eight of the twelve rats that underwent surgery were selected and paired into RAP and vehicle treatment groups. Their corresponding serum creatinines, 24-hour creatinine clearances, and urinary proteins were 0.69 versus 0.71 mg/dl, 0.91 versus 0.94 ml/min, and 205.8 versus 214.3 mg/24 h, respectively. This proteinuric CKD model enabled us to address in a CKD model of kidney injury, a known risk factor for aminoglycoside nephrotoxicity, and whether RAP could lessen the severity of kidney injury after gentamicin administration. After an additional 4-week recovery period from the nephrectomy and clamp, when serum creatinine and proteinuria were stable, gentamicin (100 mg/kg) was given i.p. daily for 5 days to five rats in two groups, saline-treated and sRAP-treated. Blood samples were drawn on days 0, 3, 4, 5, and 6, one day after the last gentamicin injection, to determine serum creatinine values, which were analyzed using a CoreLabs Analyzer Model XXZ. At the time of study, the baseline serum creatinine value for the rats in the RAP-treated group was 0.94±0.12 mg/dl and for those in the vehicle-treated group was 0.95±0.12 mg/dl.

Intravital Microscopy

Intravital 2-P microscopy was performed as previously reported.[18] Initial studies were conducted on our custom-built Olympus Flouview-1000 using a ×60 water immersion lens (numerical aperture 1.2). Later studies were conducted using a Leica Dive Multiphoton system, using a ×40 water immersion objective (numerical aperture 1.1).[16] During image acquisition, changes in laser power transmissivity were used to assure minimal saturation of endocytic accumulation to allow correct quantitation of accumulation,[25] with the exception of the TR-RAP/CBdex study, where the 40-mg/kg dose required for pharmacological efficacy caused signal saturation. For this reason, no quantitative analysis was conducted with these data. A laser transmissivity compensation curve was generated to normalize the 12-bit intensity readings for the most accurate analysis of accumulation; this has been characterized on both microscopy systems. Rats were anesthetized using isoflurane (5% induction, 1.5%–2.0% maintenance at 0.5 L/min of O_2) and monitored as previously described.[26]

Quantitative Analysis of Imaging Studies

Endocytic uptake assessments were performed as previously described.[21,27] Having standardized fluorescence values between images acquired at different laser power transmissivity allowed the results to be presented in fluorescence units/μm^2. Values were calculated using Microsoft Excel, and Student *t*-tests were conducted to identify significant differences. Dextran is a marker of CIE or fluid phase uptake, and its rapid uptake into early endosomes and progression to lysosomes with time is well-established.[2,21] Supplemental Table 1 provides the quantitative values for these studies.

Histopathology

After the 5-day gentamicin treatment, rats were saline-flushed and perfused-fixed with 4% paraformaldehyde according to institutional animal care guidelines. Kidneys were bivalved, processed into paraffin, and microtome-sectioned 3–4 μms in thickness. Paraffin sections were stained with hematoxylin and eosin, periodic acid-Schiff (PAS), and Masson trichrome. Renal histopathology was scored by one renal pathologist (C.L.P.) blinded to the treatment, as previously reported.[28,29] Two scoring systems for acute tubular injury were used, one that addressed predominantly cortical injury[30] and another that addressed medullary injury.[31] Chronic injury, including interstitial fibrosis, tubular atrophy, and FSGS, was estimated in the cortex.

Statistical Analysis

Statistical analysis (two-tailed Student *t*-test) was performed using standard statistical packages within Microsoft Excel (Microsoft, Seattle, WA) and KaleidaGraph (Reading, PA). The calculated *P*-values are presented on each graph and showed clear statistical differences between vehicle and RAP-treated conditions.

Histology Analysis

On day 6, rats were saline-flushed and perfused-fixed with 4% paraformaldehyde, followed by paraffin embedment. Four-micrometer sections were stained with H&E, PAS, or trichrome. Each sample was evaluated by the same pathologist in a blinded study, and multiple assessments were performed to evaluate kidney damage. Both a Jablonski method, to evaluate acute cortical injury, and a Colvin method, to evaluate medullary injury, were scored. In addition, fibrosis, tubular atrophy, and FSGS were assessed.

Results

Lrpap1 (RAP) Filtration and Internalization by Renal PTs

Understanding the alterations of the subcellular physiologic mechanisms affected by Lrap1 (RAP), which induce alterations in PT endocytic function, may prove beneficial, particularly if they are reversible. To address these questions, a Texas Red conjugate of Lrap1 (TR-RAP) was used to study PT handling and accumulation characteristics *in vivo* in the kidney using multiphoton microscopy. In these initial studies, a single iv bolus of 3 mg/kg was given to MWF rats, which have surface glomeruli. The kidney processing of TR-RAP was followed for 2 hours in the microscope stage. The tracer dose was selected because higher doses of this 1:1 dye:protein conjugate quickly saturated PT intracellular vesicles containing the marker, making interpretation difficult at latter time points. The set of micrographs in Figure 1 focuses on a single glomerulus and S1 segment before and after infusion of RAP. TR-RAP filtered across the glomerulus rapidly into Bowman's space. Binding to the apical brush border in the S1 segment (arrow) occurred rapidly, within 20 seconds (Figure 1B). Enrichment of TR-RAP at the apical brush border progressed from brush border binding to early uptake localized within small subapical vesicles occurring at 4 minutes (Figure 1C). Continued tracking of the accumulated marker in the same region showed progressive migration of the marker from the brush border region to distribution throughout PT cells within structures associated with the endocytic pathway. These bright, vesicular endosomes form vesicular-tubular structures that extend deeper into the PT cells (Figure 1E, 45 minutes after infusion) and are seen extending toward the basolateral membranes (Figure 1F, 2 hours after infusion). The inset in Figure 1F clearly shows the connected vesicular-tubular structures. The dose used in this study was found to accumulate in only a few of the PT segments studied, mainly S1 segments. The higher magnification micrographs in Figure 1, C, E, and F show an S1 segment with notable uptake of TR-RAP surrounded by PT segments whose fluorescence remained unchanged from the background image. A low-power micrograph in Figure 1D further validates this finding in the area surrounding the observed region. This observation is consistent with the lack of accumulation of filtered TR-RAP in the lumens of dt (Figure 1D) and indicates that retrieval of TR-RAP occurred entirely in early PT segments. We do not know whether giving a larger dose would have resulted in downstream PT segments taking up RAP.

Administration of RAP Reduces Clathrin-Mediated and Clathrin Independent Endocytosis

Having established RAP is rapidly filtered and traffics along the endocytic pathway in kidney S1 PTs, we next set out to determine if its presence affected fluid phase and receptor mediated endocytosis. To accomplish this simultaneously, we used a CB conjugated 10-kDa amino dextran (CBdex), selected as the CIE or fluid phase marker, and a 1:1 dye:protein conjugate of TR-RSA as the CME marker. The two fluorophores have spectral emissions that are easily separated when simultaneously excited at 800-nm wavelength, two-photon illumination. Data from S1 segments (distinguishable by their connection to the glomerulus/Bowman's space) and other outer cortical PT segments (S1's not having a clear glomerular opening and S2s) are reported separately. A dose of 40 mg/kg nonfluorescent RAP or the same volume of the saline vehicle was administered approximately 10 minutes before infusion of the CIE and CME markers. It is important to note the 3-mg/kg dose used for the *in vivo* trafficking studies was insufficient to induce the reduction in uptake (data not shown), but served as a tracer dose to understand kidney handling. The results for the CBdex CIE marker showed a significant decrease (*P = <0.05) in PT fluorescence uptake of both markers at each time point in RAP-treated rats, in both S1 and cortical PT segments. The micrographs in Figure 2 show images for the CBdex channel acquired 60 minutes after infusion. In the vehicle-treated group (Figure 2A), robust punctate uptake of CBdex is seen in the S1 PT segment (adjacent to the glomerulus—G) and surrounding PT segments. By contrast, the PTs in the RAP-treated image (Figure 2B) showed reduced internalization predominantly in the S1 segment, which is where the TR-RAP exhibited the greatest accumulation in the initial trafficking studies (Figure 1). The quantitative data from the uptake studies confirmed that the greatest reduction in uptake of the CIE marker occurred in the S1 segments (Figure 2C), with a nearly six-fold difference across the time points, except for the 30-minute time point. Other outer cortical PT segments (Figure 2D) also showed a significant decrease in uptake at all time points with a maximum two-fold reduction occurring at the 30-minute time point.

Analysis of the micrographs for the CME marker TR-RSA again showed a similar pattern with a significant reduction in uptake after RAP administration occurring in the PTs. The micrographs in Figure 3, obtained 60 minutes after infusion of the CME marker, show the TR-RSA channel for the vehicle-treated and RAP-treated rats in Figure 3, A and B, respectively. This is the same region showing the CIE marker in Figure 2. In these images, however, the greatly reduced glomerular permeability for TR-RSA causes retention within plasma, highlighting the peritubular blood vessels and glomerular capillary loops (G=glomerulus) unlike the images for the smaller dextran, which is filtered freely across the glomerulus. In the PTs, the presence of TR-RSA accumulation within the endocytic pool seen in the vehicle-treated rats (Figure 3A) is greatly reduced by RAP treatment (Figure 3B). The quantitative data from the TR-RSA images are shown in Figure 3, C and D for the S1 and PTs, respectively. The rats in the RAP group had on average a 2–2.5-fold reduction in the 15, 30, and 60-minute time points, with the reduction in uptake being more pronounced in the S1 segments. The reduction in TR-RSA uptake in PT segments increased over time from 1.3-fold to 2.1-fold. This finding is consistent with the results seen for dextran. The glomerular sieving coefficient was also quantified for TR-RSA, and no significant difference was measured (+vehicle=0.0158±0.0036, +RAP=0.0163±0.0042, P = 0.6782).

RAP Exposure Reduces PT Gentamicin Uptake

The ability to minimize the effects of nephrotoxic drugs on renal tubular epithelia could have far reaching clinical implications. The PTs are the site of cellular uptake after administration and glomerular filtration. The aminoglycoside antibiotic gentamicin was chosen as an example of a

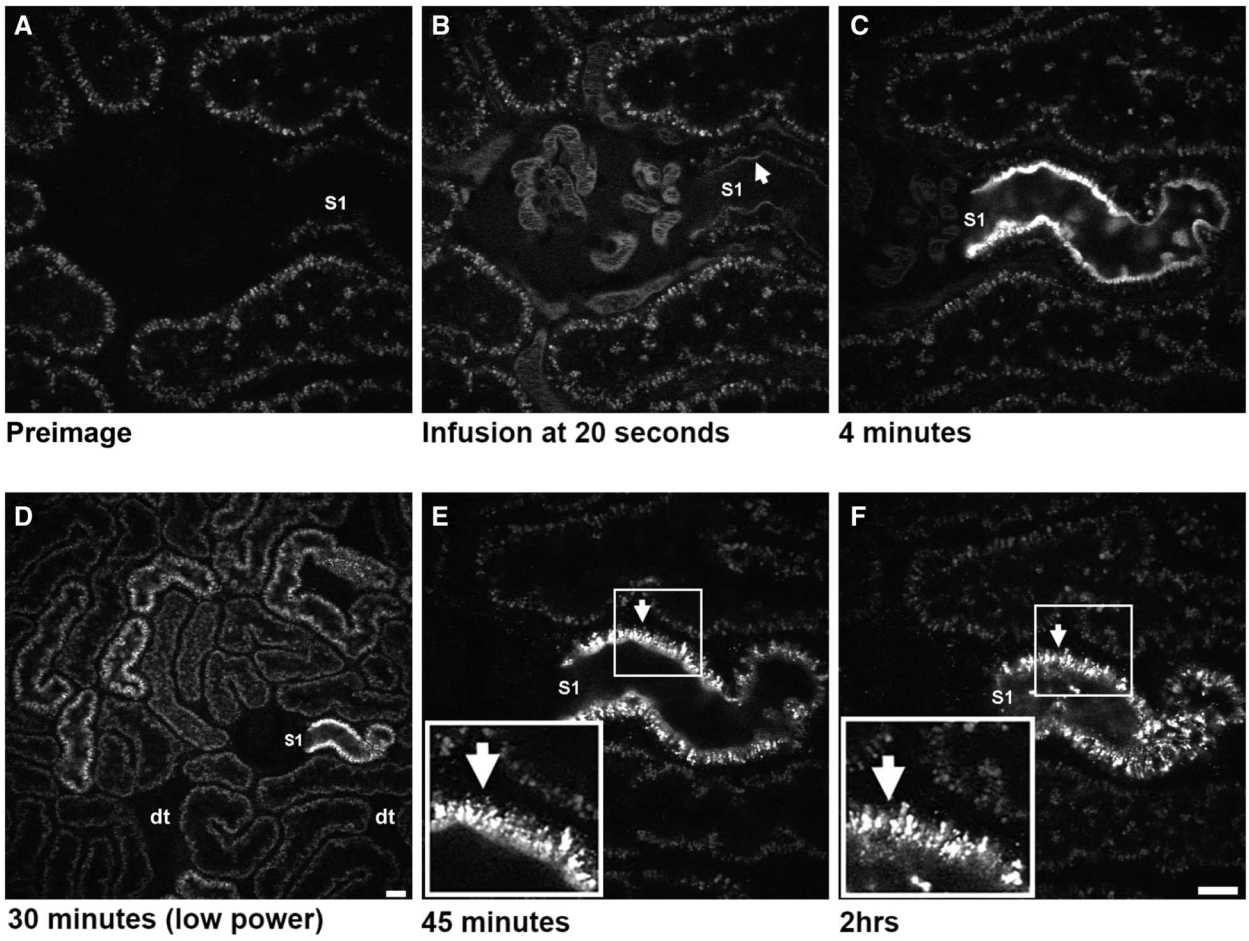

Figure 1. TR-RAP is rapidly internalized by PT cells. MWF rats, a rat strain expressing surface glomeruli, were given an iv bolus of TR-RAP at a dose of 3 mg/kg. (A) Preimage of the Texas Red channel in black and white. The empty center is a glomerulus surrounded by PTs in cross-section in this series of single plane images. The autofluorescence in the lysosomes appear as faint punctate structures associated with the lysosomes; note the reduced autofluorescence seen in the S1 segment followed in this figure. (B) Infusion and filtration of the TR-RAP is seen in a snapshot obtained at 20 seconds into a time series of the infusion. Individual glomerular capillary loops are seen in the center, with the circulating red blood cells outlined by the TR-RAP in the plasma. The rapidly filtered TR-RAP is seen binding to the apical brush border of the S1 segment (arrow). (C) Binding and enrichment of TR-RAP at the apical brush border continues, where small early endosomes appear internalized from the bound fraction pool (see inset). (D) Distribution of the fluorescent bolus at this dose appeared solely within the endocytic compartment of PT cells in early segments. No evidence of TR-RAP was seen within the tubular lumen of dt, suggesting all the infused compounds were internalized by the PTs. Note, dt lack autofluorescence in stark contrast to PTs. (E and F) The same S1 segment shown, this time at 45 minutes and 2 hours after infusion, respectively. The inset images in these panels show in greater detail the trafficking of internalized TR-RAP as it migrates deeper into the cells in vesicular-tubular structures with some of these extensions nearing the basolateral membrane (Bar=20 μm). These studies used only tracer amounts of RAP conjugated to Texas Red. Note, the S1 group is identified/defined as PTs with a clear glomerular opening determined by two-photon microscopy.

nephrotoxic drug to determine whether administration of RAP reduced proximal tubule cell uptake and provided kidney functional protection. A Texas Red conjugate of gentamicin (TR-G) was used to study this potential benefit. Following the protocols established in the previous studies, MWF rats were given the same 40-mg/kg doses of RAP 10 minutes before a single bolus infusion of TR-G, with images acquired at 15, 30, and 60 minutes after infusion. The fluorescence data were normalized as described in the previous uptake studies of the CME and CIE markers and analyzed. The results from these studies showed significantly reduced PT accumulation of TR-G in the RAP-treated rats. Notably, increased endocytic inhibition was observed with sRAP compared with RAP, as expected. Photomicrographs obtained at 60 minutes after TR-G infusion show uptake along the endocytic pathway with accumulation occurring in the lysosomes in vehicle-treated rats, as shown in Figure 4A. The typical yellow-orange autofluorescence found in the PT lysosomes now displayed a bright red fluorescence because of the accumulated TR-G in both S1 and other outer cortical PT segments. The RAP-treated group again had markedly reduced uptake, which was more pronounced in the S1, which would normally see the bulk of any filtered aminoglycoside. The S1 segment seems to display only the yellow-orange autofluorescence and little to no TR-G accumulation. One observation seen in the RAP-treated group is the continued presence of TR-G binding to the apical brush border membrane, predominantly in the PT segments (* Figure 4B).

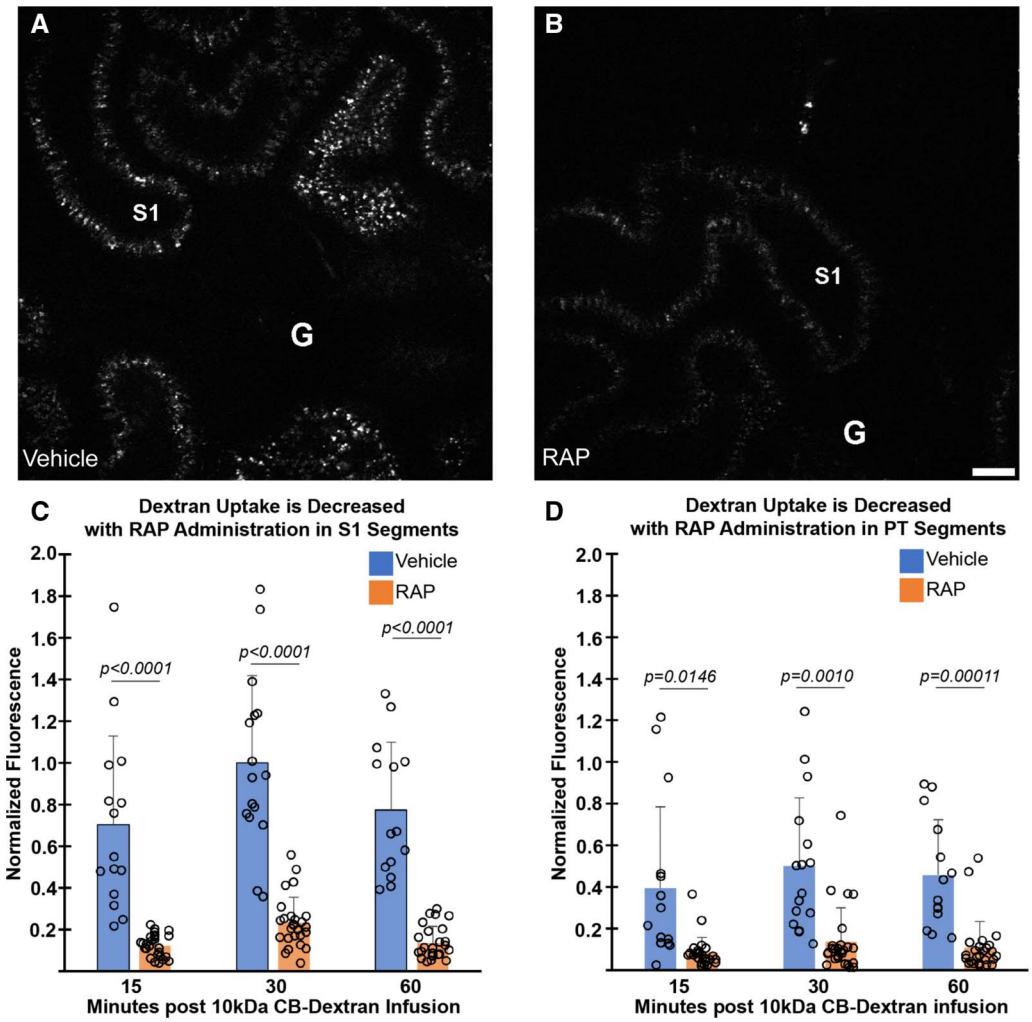

Figure 2. Unlabeled RAP significantly decreased accumulation of fluorescent 10-kDa dextran in PT cells. Ten minutes after infusion of nonfluorescent RAP at 40 mg/kg or the normal saline vehicle, a single bolus of TR-RSA and 10-kDa CBdex was administered and images were obtained at approximately 15, 30, and 60 minutes after infusion. (A and B) Single plane images obtained at 60 minutes of the vehicle-treated and RAP-treated rats, respectively. (A) The S1 segment in the vehicle-treated rat accumulated more of the 10k CBdex than the S1 segment in the RAP-treated rat (B). This reduction also occurred in later segments of PT. (C and D) Quantitative analysis of fluorescent uptake between the RAP and vehicle groups, graphed for both S1 and non-S1 PT segments, respectively. (C) Normalized dextran accumulation in the S1 segments of PTs; peak fluorescence occurred in the vehicle-treated rats at the 30-minute interval. Pretreatment with RAP produced a significant reduction in internalization of the dextran fluid phase marker at all time points examined, when compared with the vehicle-treated rat group. The reduction of dextran uptake in RAP-treated rats is well over five-fold in the S1 segment (C); this is lessened to a two-fold decrease in other PT segments in RAP-treated rats (D). Supplemental Table 1 presents the quantitative values for C and D and specific *P*-values are provided within the graph (G=glomerulus, Bar=20 μm). Note, the S1 group is identified/defined as PTs with a clear glomerular opening determined by two-photon microscopy and PT comprise S1 PTs without a clear opening and S2 PT segments. These studies used RAP.

Presumably, this may be because of the high-capacity, lower affinity binding of gentamicin to the PT apical membranes.[22] The analyzed uptake data are displayed in Figure 4, C and D for the S1 and PT segments, respectively, showing accumulation in both S1 and other outer PT segments. The decrease in TR-G fluorescence for the RAP-treated rats was approximately a two-fold reduction.

RAP-Induced Reduction of Endocytic Function is Reversible

The next studies were conducted to see whether the effect of RAP on PT endocytosis was reversible. sRAP was administered at the same dose of 40 mg/kg and the same fluorescent CME and CIE markers, given either 10 minutes or 4 hour + 10 minutes after RAP infusion. Given the greater uptake of RAP in S1 PTs (Figure 1) and increased inhibition of uptake by sRAP over RAP (Figure 4), recovery in the S1 PTs would be expected to be delayed relative to the downstream PTs. Figure 5, A and B presents paired single plane images for CBdex and TR-RSA uptake collected 70 minutes after sRAP infusion. The circulating TR-RSA (Figure 5B) within the capillary loops of the glomerulus (G) and surrounding peritubular vessels should be noted. The S1 segment (S1) and surrounding PTs (*) fail to internalize either marker, with the PTs having their

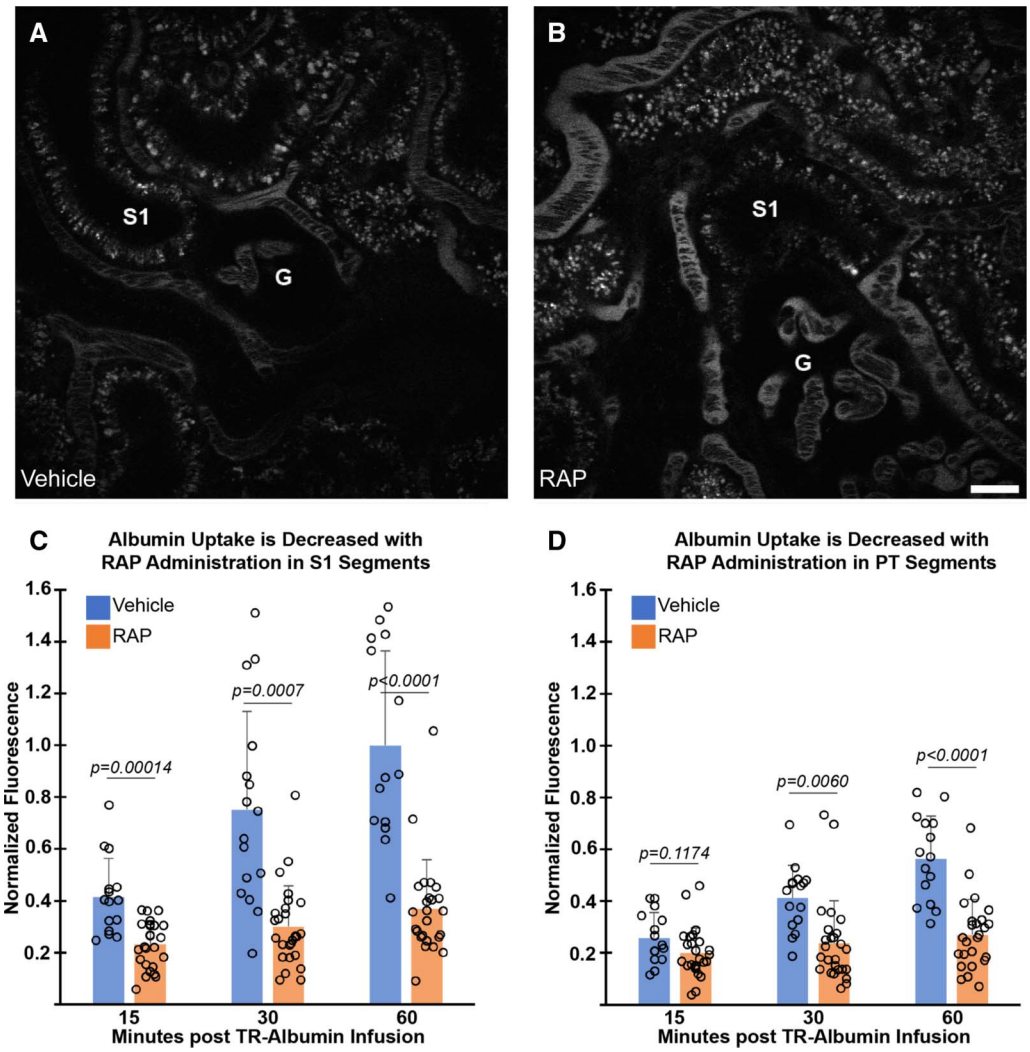

Figure 3. RAP reduces endocytosis of filtered TR-albumin. TR-RSA, coadministered with the studies outlined in Figure 2, showed significant reduction in uptake for this marker of CME in RAP-treated rats. (A and B) Single plane images of TR-RSA distribution at 60 minutes after infusion for the saline vehicle and RAP-treated groups, respectively. The first noticeable difference is the vascular retention of the TR-RSA fluorescence at 60 minutes due to the approximately 66-kDa molecular weight, which fills the plasma and highlights the capillary loops of the glomerulus (G). Endocytic internalization of TR-RSA can be more easily visualized in the S1 segment, which receives the highest concentration at a slower rate of filtration. (A) The S1 segment demonstrates this in the vehicle-treated rats as bright, punctate endosomes and lysosomes. (B) The S1 segment for the RAP-treated rat shows a marked reduced uptake in comparison. (C and D) The quantified, normalized data comparing TR-RSA uptake between the two groups in the S1 and PT segments, respectively. The peak value for TR-RSA accumulation occurred at the 60-minute time point in the vehicle-treated group. The RAP-treated rats again had a significant reduction, with the internalized albumin for all the time points analyzed in both S1 and PT segments. A reduction of approximately 2–2.5-fold occurred in the 30- and 60-minute time points for the S1 and nonsegments. Supplemental Table 1 presents the quantitative values for C and D and specific *P*-values are provided within the graph (Bar=20 μm). Note, the S1 group is identified/defined as PTs with a clear glomerular opening determined by two-photon microscopy and PT comprise S1 PTs without a clear opening and S2 PT segments. These studies used RAP.

characteristic autofluorescence unchanged. By this time, the CBdex has cleared the vasculature and is not readily seen. Quantification of fluorescence uptake showed complete inhibition at this early time point consistent with the inhibition of gentamicin observed by sRAP at 60 minutes after infusion (Figure 4). Figure 5, C and D presents paired single plane images for CBdex and TR-RSA collected 5 hours and 10 minutes after sRAP infusion. At this time point, uptake of both CBdex and TR-RSA was observed. However, as expected, increased recovery was observed for both CBdex and TR-RSA in PTs downstream from S1, which endocytosed the greatest amount of sRAP. Normalized fluorescence for TR-RSA uptake was 0.38±0.079 for S1 and 1±1.2 for other PTs while for CBdex uptake, S1 was 0.12±0.06 and for other PTs, was 1±1.41. The variability in recovery in the outer ortical S2 PTs may relate to glomerular proximity because those tubules were more distant with lower concentrations of sRAP available. Importantly, the level of uptake at 5 hours and 10 minutes is consistent with a partial recovery and provides support for daily RAP dosing to evaluate protection from aminoglycoside toxicity. Increased uptake in downstream PTs versus S1 is

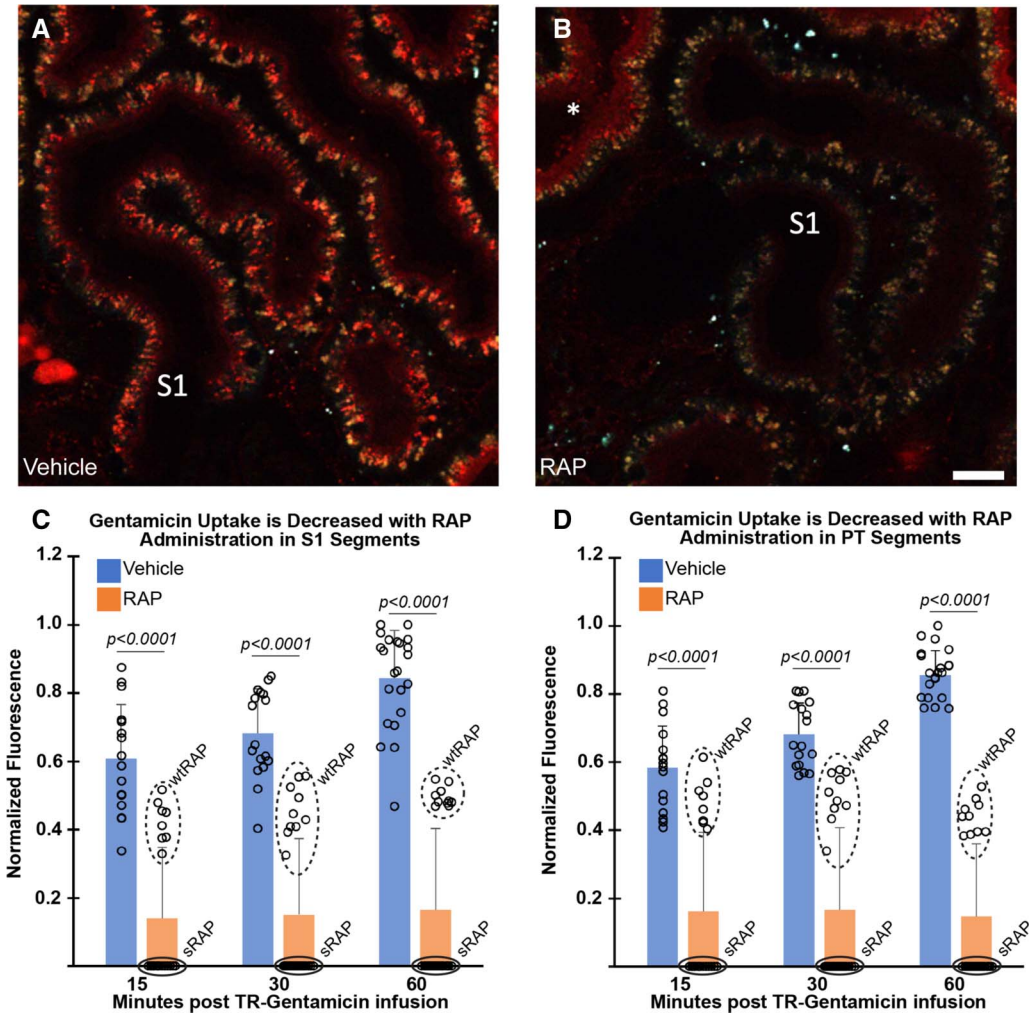

Figure 4. Administration of RAP before infusion of a fluorescent aminoglycoside reduces PT uptake. A TR-G (red) was given as a single bolus in rats, which were given either saline vehicle or nonfluorescent RAP 10 minutes before infusion, and images were obtained at approximately 15-, 30-, and 60-minutes after infusion. (A and B) The images are obtained 60 minutes after TR-G infusion and represent vehicle-treated (A) and RAP-treated (B) rats. A comparison of the S1 segment shows a reduction of TR-G uptake in the RAP-treated rats (B) with the S1 segment in the vehicle rats (A). The RAP-treated group retained binding of TR-G to the brush border of PTs even 60 minutes after infusion (B, *). Quantitative analysis of the images was conducted on fluorescent uptake data normalized to the peak value; the 60-minute time point for the S1 segments of the vehicle group values. The S1 (C) and other PT (D) segments in the RAP-treated rats both had a significant reduction in accumulation of TR-G of approximately two-fold. Supplemental Table 1 presents the quantitative values for C and D; specific *P*-values are provided within the graph. Note, the S1 group is identified/defined as PTs with a clear glomerular opening determined by two-photon microscopy and PTs comprise S1 PTs without a clear opening and S2 PT segments. These studies used both RAP and sRAP.

consistent with a recent study by the Hall group showing that compensatory uptake in later regions of PTs occurs to prevent urinary loss.[32]

RAP Treatment Minimizes Nephrotoxicity

Having established reduced trafficking of TR-G into renal PTs, we next moved on to study this effect in a more real-world model of gentamicin nephrotoxicity.[22] We selected a CKD model, and the rats were paired into two groups with similar serum creatinine and 24-hour proteinuria levels. For the aminoglycoside toxicity model, we selected a dose of 100 mg/kg of native gentamicin delivered in a single dose i.p. daily for 5 days. The rats received a saline vehicle or sRAP injection (40 mg/kg) through the tail vein before the i.p. injection of gentamicin. Loss of kidney function was determined by the elevation in serum creatinine concentration over the course of several days of treatment. The CKD group treated with vehicle (rats 4–8) had no elevation in serum creatinine during the first 3 days of the study, but showed a highly significant increase on days 5 and 6 of the study, with day 6 having an over five-fold increase above baseline (0.95±0.12 mg/dl vs 5.4±0.80 mg/dl, $P < 0.01$). The sRAP-treated group (rats 1–4), by contrast, showed no statistical elevation in serum creatinine ($P > 0.05$); these rats had a marginal increase of approximately 1.6-fold at day 6 (0.94±0.12 versus 1.53±0.49; Figure 6).

Twenty-four–hour quantitation of creatinine clearance and urine protein on day 6 confirmed the protective effect of sRAP on the treated animals (rats 1–4) versus the vehicle

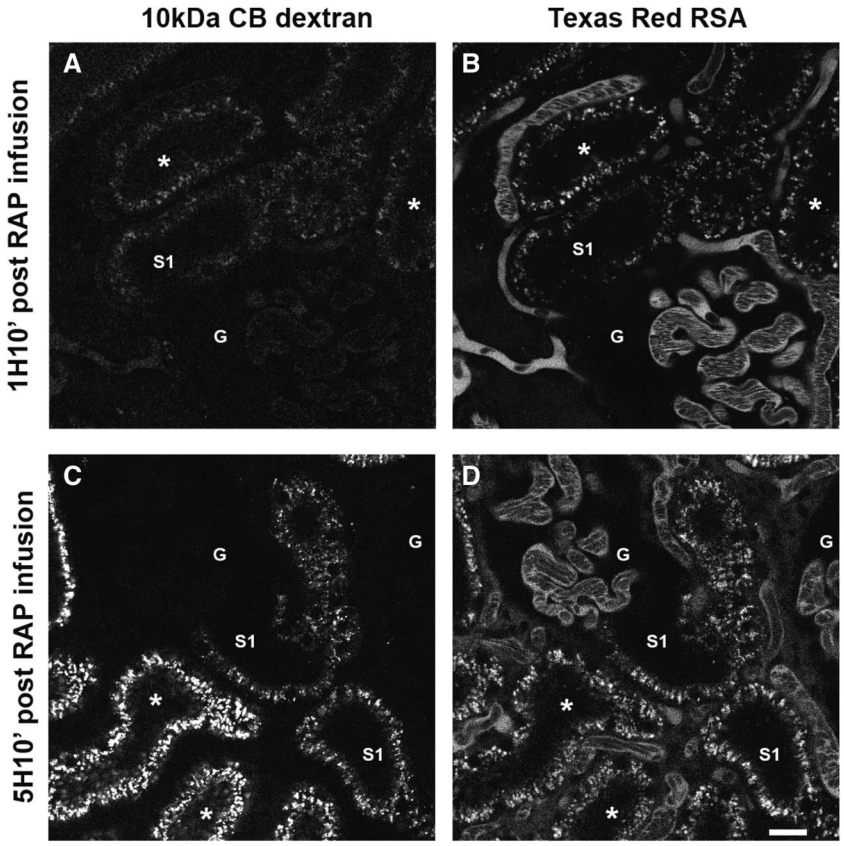

Figure 5. Inhibition of PT endocytosis after RAP administration is reversible 4 hours after an initial bolus infusion. In these data, either saline vehicle or nonfluorescent RAP was administered at a dose of 40 mg/kg in MWF rats. Rats were then imaged for accumulation of TR-RSA and a CB 10-kDa dextran (CBdex) administered at either 10 minutes or 4 hours and 10 minutes after RAP infusion. (A and B) Single plane images for the CBDex and TR-RSA, respectively. A rat imaged 60 minutes after infusion of the fluorescent markers in the 10-minute post-RAP group follows the same protocol as in Figures 2 and 3. (A) The CBdex channel. The PTs have very little autofluorescence in the lysosomes in the blue channel, which remains virtually unchanged due to the lack of CBdex accumulation by the tubular epithelia. The S1 segment (S1), other PTs (*), and glomerulus (G) are seen here and in the corresponding TR-RSA image (B). The TR-RSA is retained within the plasma highlighting the vasculature surrounding the PTs and the capillary groups of the glomerulus (G). (B) Texas Red RSA, which is normally avidly accumulated in the endocytic compartment of PTs (S1, *), is absent . At the total elapsed time of 70 minutes after RAP infusion, inhibited endocytic uptake in PTs persisted for both fluorescent probes. (C and D) On the contrary, single plane images for CBdex and TR-RSA, respectively, show uptake of both fluorescent probes in these regain of function studies. This set of images were obtained in rats with an elapsed time of 4 hours and 10 minutes after RAP infusion and 60 minutes after a single bolus infusion of both probes. The S1 PT segments, adjacent to their glomeruli (G), show accumulation of both CBdex (C) and TR-RSA (D), while PTs (*) appear to show more accumulation of the CBdex (Bar=20 μm). These studies used sRAP.

group (rats 4–8). Twenty-four–hour creatinine clearance in the RAP-treated rats was 0.49±0.16 ml/min while in the vehicle-treated group, it was 0.09±0.07 ml/min ($P < 0.01$, Figure 7A). Twenty-four–hour urinary protein/GFR had increased to 487.6±193.7 mg/GFR in the RAP-treated group and 2512.3±362.0 mg/GFR in the vehicle-treated group ($P < 0.01$, Figure 7B).

Figure 8 contains representative PAS-stained kidney sections from vehicle (saline) or RAP (treated) animals from both the superficial cortex and the deep cortex. Evidence of chronic histologic changes was observed in both groups and was similar. Table 1 presents no clear correlation between acute injury histologic changes, and the physiology data were observed, except for the number of tubular casts/high-power field that were reduced in RAP-treated rats ($P < 0.05$). In addition, acute cortical injury total Jablonski scores (modified scores of 3A, 3B, 3C, and 4 into a numerical scale of 3, 4, 5, and 6, respectively) resulted in a P value of 0.0857 when comparing the RAP-treated value of 4.25±3.59 with the vehicle-treated value of 8.25±1.5 (n=4 for each group).

Discussion

The nephrotoxicity of many endogenous and exogenous substances is mediated by PT reabsorption after glomerular filtration. This phenomenon has been understudied as a cause of AKI, but there is now renewed interest with many small molecule therapies being developed having nephrotoxicity as a clinically relevant side effect.[1] The mechanism of aminoglycoside toxicity has been studied extensively, and it is known that the positive charge of aminoglycosides influences binding and subsequent endocytosis.[33–36] After endocytosis, aminoglycosides can be transported to the lysosome or travel retrogradely

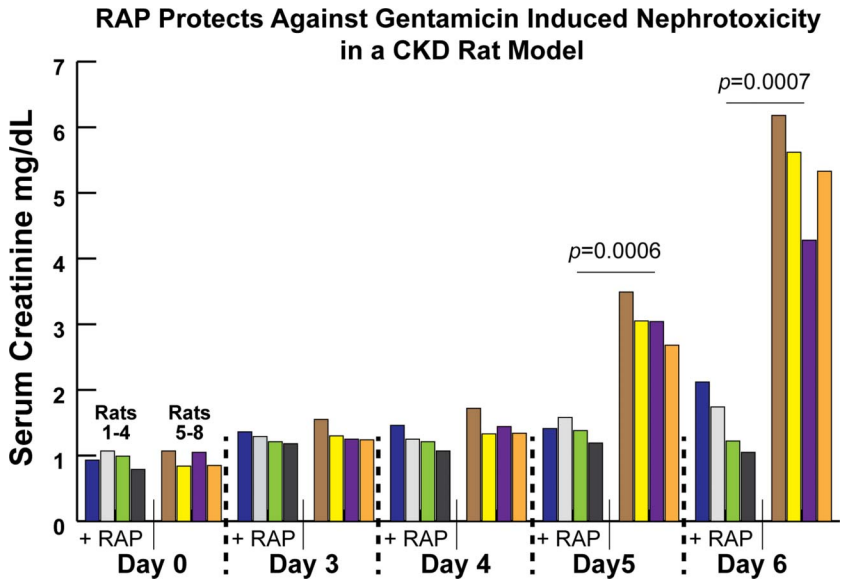

Figure 6. A 5-day study of gentamicin nephrotoxicity in a rat CKD model showed RAP administration improved renal function. The CKD rats generated for the study were divided into two groups having nearly identical reduced renal function parameters. All rats received gentamicin (100 mg/kg) daily, i.p. for 5 days. Before each injection, rats received saline vehicle or 40 mg/kg RAP using tail vein injections. Blood was drawn at days 3, 4, 5, and 6 (1 day after the last injection) and analyzed for serum creatinine. The data show that the vehicle-treated group (rats 5–8) had a significant reduction in renal function at days 5 and 6, as determined by a 5.6-fold increase in serum creatinine at day 6, specific *P*-values are provided within the graph. By contrast, the RAP-treated group (rats 1–4) reported only a 1.6-fold increase at day 6. These studies used sRAP. Each colored bar represents the value for a rat at the reported time point ($n=4$).

through the Golgi apparatus and even be released into the cytosol.[37–39] Once free in the cytosol, they mediate toxicity and damage to the mitochondria[40,41] and likely other subcellular organelles. Given the multiple PT pathways available to these small positively charged molecules, the potential for multiple yet unknown modifying interactions exist.

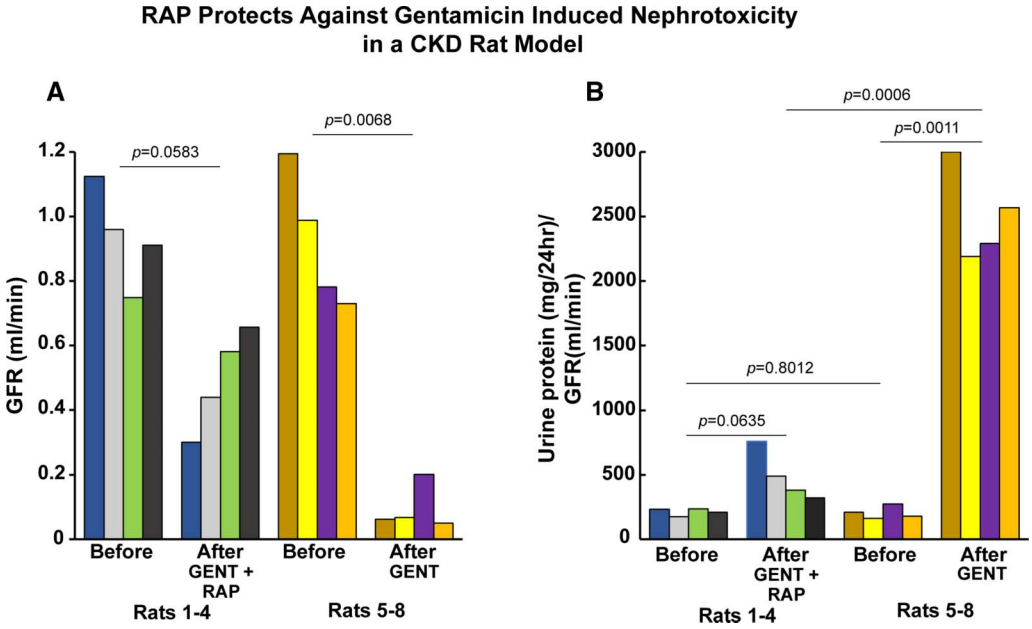

Figure 7. RAP minimizes gentamicin nephrotoxicity-induced decline in GFR and increases in proteinuria after 5 days of gentamicin treatment. (A) The result of gentamicin treatment on the 24-hour clearance of creatinine, as a measure of GFR. Both groups had a decrease in GFR, but the reduction in the RAP-treated group was far less. (B) Urinary protein excretion is factored for GFR and shows RAP minimized the increase in 24-hour protein. Each colored bar represents the value for a rat at the reported time point ($n=4$).

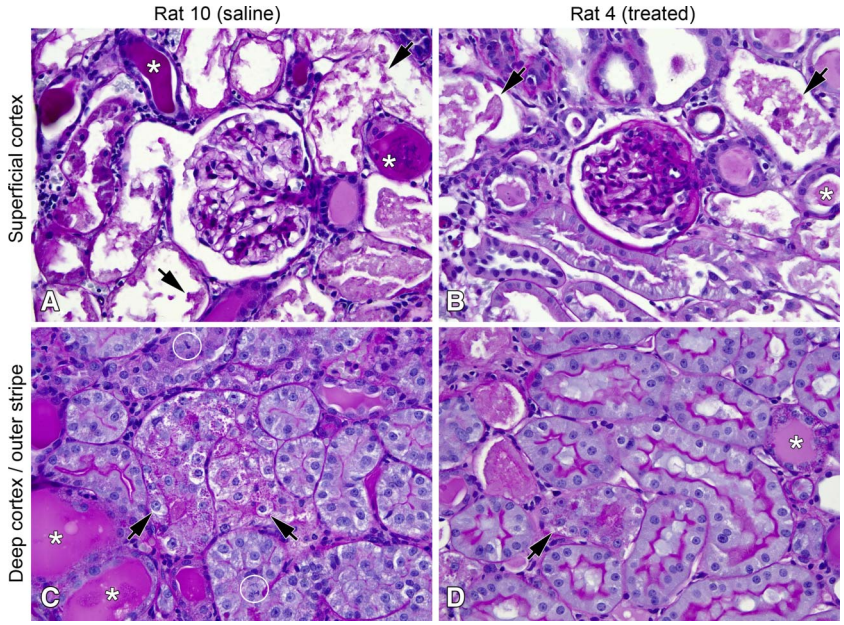

Figure 8. Light microscopy: formalin-fixed, paraffin-embedded sections of the kidney were stained with PAS. (A) A representative sampling of the superficial renal cortex from a saline-treated/sham rat shows extensive acute tubular injury with detachment of the epithelium from tubular basement membranes (arrows) and intraluminal proteinaceous casts, including some containing cell debris (*), compared with a less extensive but similar injury pattern in the treated rat (B). Representative areas from the outer strip of a saline-treated rat (C) show the renal tubule epithelium with loss of brush borders and cytoplasmic vacuolization and protein reabsorption droplets (arrows). Mitotic activity (circles) and intraluminal proteinaceous casts (*) are noted. Similar features are seen in the treated rat (D) but are less intense in this image.

PT cells, especially the S1 segment, have very rapid endocytosis that is responsible for the uptake of numerous filtered substances (*i.e.* proteins, peptides, vitamins, and drugs). In addition, while trafficking to lysosomes is common, some molecules traffic to the Golgi apparatus and endoplasmic reticulum and can also be trancytosed.[3,18,41–43] Consequently, protective therapies to limit aminoglycoside PT uptake and reduce the resultant damage have been pursued. Some approaches, such as calcium or lysine infusion to minimize PT apical binding and endocytic uptake, are clinically impractical.[34] Some benefit has been shown for cilastatin, although its administration may have unwanted consequences due to its dehydropeptidase I inhibitory properties.[44,45]

Because much is still unknown concerning the interplay between CME and CIE in the PT, these studies were focused on further evaluation of these two endocytic mechanisms and the effect of RAP on them quantified by intravital microscopy methods in the MWF rat model.[2] This approach affords the unique opportunity to visualize, in real time, both filtration and PT uptake and trafficking.[46] RAP has been shown to partially inhibit PT accumulation and even toxicity of several toxins; however, the mechanism has never been investigated using intravital microscopy.[11,13,14,47] We also chose to evaluate the recently described sRAP, which does not dissociate in the acidic endosomes, thus extending the ligand-binding inhibition for this form and possibly offering improved reduction of nephrotoxin uptake.[15] Furthermore, it is important to state that RAP has many identified and potential protein interactors, most of which are present in PTs (BioGRID [https://thebiogrid.org/] identifies 137 protein associations).

TR-RAP was rapidly endocytosed by PTs after filtration with S1 segments taking up more than other cortical PT cells. We do not know whether this was because of the lack of TR-RAP exposure to downstream PTs or their inability to take it up. Most of this RAP trafficked to large punctate structures consistent with lysosomes. Administration of RAP before albumin infusion resulted in a significant reduction in PT albumin uptake as expected because RAP can prevent ligand binding to cubilin and megalin.[48,49] Since RAP is normally found as an intracellular protein, iv infusion as used here, and by other investigators, can be expected to lead to interactions not normally encountered. Consequently, the exact mechanism of how RAP inhibits CME will require further investigation.

The effects of RAP on CIE were also addressed. Before RAP infusion, the uptake of the CIE marker, 10-kDa dextran, was greater in S2 than in S1 cells, and the CME marker albumin was higher in S1 than in S2 cells. This is in agreement with previous studies showing that S2 cells are known to have increased uptake by fluid phase endocytosis.[50] Interestingly, RAP affected both CME, as expected, and CIE, which was not expected. This may indicate that megalin may exert a permissive function in allowing CIE, but this remains to be determined. However, the effect of RAP on endocytosis was partially reversible at 4 hours, with significant recovery observed by 4 hours most notably in downstream PTs. We did not quantify later time points to determine whether full recovery of endocytosis occurred in S1 PTs. Notably, daily injections of sRAP for 5 days did not result in histologic changes or apparent PT disfunction for protein endocytosis.

Table 1. Renal pathologist analysis of vehicle and RAP-treated kidneys.

Rat Number	Acute Cortical Injury, Jablonski	Medulla Injury, Colvin	Percent Interstitial Fibrosis	Tubular Atrophy	FSGS	Hyaline casts/ten 20× High-Power Fields (protein casts w/o cells)	Other
+RAP							
1	3B, 3C	2	5	<10%	17/100	73	Upper two-thirds of the cortex shows greatest acute injury
4	3C	3	15	11%-33%	23/100	29	Upper one-third of the cortex shows greatest acute injury, variable
5	2	1	5	<10%	9/100	26	Patchy necrosis in outer one-third of the cortex
8	1	1	10	11%-33%	2/100	22	One of the better looking kidneys
Vehicle							
3	4	3	10	<10%	28/95	52	One of the worst: majority of the cortex shows acute injury
6	3B, 3C	2	5	<10%	2/100	75	Upper half of cortex shows greatest acute injury
10	3B, 3C	1	10	11%-33%	4/100	87	Upper half of the cortex shows greatest injury
12	3B, 3C	1	5	<10%	3/100	102	Upper half of the cortex shows greatest acute injury

Acute injury scored using a modified Jablonski method because that system does not fit the pattern of injury observed. Hematoxylin and eosin and PAS slides were scored to address injury to cortical proximal tubules. 1=mitosis and necrosis of individual cells; 2=necrosis of all cells in adjacent PCT, with survival of surrounding tubules; 3A=necrosis in the inner cortex (distal one-third of PCT with a band of necrosis extending across the inner cortex); 3B=necrosis in the middle cortex middle one-third of PCT with a band of necrosis extending across; 3C=necrosis in the outer cortex (superficial third of the cortex from capsule inward); 4=necrosis affecting all three segments of the PCT (full-thickness cortex). Medulla injury scored using the method of Colvin, which addresses an injury in the outer medulla (percentage of tubules in the outer medulla with epithelial cell necrosis or necrotic debris). 0=none; 1=<10%; 2=10%-25%; 3=26%-75%; 4=>75%. Interstitial fibrosis was estimated from scoring of trichrome and PAS slides as a percentage of cortex. Intraluminal hyaline casts in tubules were counted in the superficial cortex of PAS-stained sections. There was a statistical difference between the two groups, with the treated group having fewer casts ($P<0.05$). Representative histopathology images are shown in Figure 8. RAP, receptor-associated protein; FSGS, focal segmental glomerulosclerosis; PAS, periodic acid-Schiff.

Because RAP inhibited both CME and CIE uptakes, it was reasonable to hypothesize that prior administration of RAP could limit PT uptake of many different nephrotoxins and thus prevent PT cell injury. To directly answer this question, we chose to look at gentamicin nephrotoxicity using a sensitive model. Rats have a large renal reserve capacity as evidenced by the fact that unilateral nephrectomy does not alter their baseline serum creatinine. Therefore, to show an increase in serum creatinine requires more than a 50% reduction of kidney function. However, with loss of function, as in a CKD model, sensitivity to further loss of function is increased as it is clinically. The model of right unilateral nephrectomy and simultaneous left ischemic clamping in MWF rats resulted in rats with a stable serum creatinine of approximately 1.0 with increased proteinuria. This model proved advantageous in testing whether RAP given before a nephrotoxin could reduce nephrotoxicity. In fact, in the absence of RAP, a 5.6-fold increase in sCr (5.3±0.80) occurred while with RAP administration, sCr only rose 1.6-fold (1.5±0.49, Figure 6). This was associated with a large decrease in GFR in the vehicle-treated group and a much smaller decline in the sRAP-treated group (Figure 7A). Proteinuria, factored for GFR, also increased dramatically more in the vehicle-treated group (Figure 7B), implying more PT disfunction for protein and albumin reabsorption.

The largest changes in kidney function did not correlate statistically with changes in histology. In this CKD model, there are moderate-to-severe histology changes at baseline, likely making identifying acute changes more difficult. Only the number of intralumenal casts/high-power field reached statistical significance ($P < 0.05$), with an n of 4.

The rapid endocytosis of RAP in PTs and rapid initiation and reversible inhibition of CME and CIE will, as we hypothesized, allow adequate time for filtration and urinary clearance of small molecules, those that can clear within approximately 90 minutes (RAP's apparent PT half-life when administered iv). Furthermore, because the effect of endogenous RAP is reversible and because it is a normal cellular protein, other unforeseen harmful consequences are likely reduced. Consequently, we believe RAP administration before the infusion of an exogenous nephrotoxin, which undergoes PT endocytosis, could be used to minimize and or totally prevent PT cell injury. This approach could also limit uptake of filtered myoglobin in patients with high levels of myoglobinemia or free hemoglobin released during muscle injury and hemolysis, respectively.

Disclosures

B.A. Molitoris reports the following: Employer: Consultancy: Akebia, AM Pharma, CSL Behring, Ionis, Rayze Bio, Seagan, and Tamarix; Ownership Interest: FAST BioMedical; Research Funding: Ionis, NIH-Research Grants, Razebio, and Segen; Patents or Royalties: Provisional patent entitled Alleviating Drug Nephrotoxicity No. 63/337,798. FAST BioMedical, GFR and plasma volume measurement, Indiana University C1 and C2 Gentamicin and Soluble Thrombomodulin, Verterans Administration siRNA for CKD; and Advisory or Leadership Role: Akebia (SAB), AM Pharma (DSMB comm.), CSL Behring (DSMB), FAST BioMedical, and Ionis (DSMB). C.L. Phillips reports the following: Ownership Interest: Alphabet, Disney, and Wells Fargo. R.M. Sandoval reports the following: Consultancy: FAST Biomedical and TdB Consultancy, Uppsala, Sweden; Patents or Royalties: Provisional patent entitled Alleviating Drug Nephrotoxicity No. 63/337,798. FAST BioMedical. M.C. Wagner reports the following: Patents or Royalties: Provisional patent entitled Alleviating Drug Nephrotoxicity No. 63/337,798. The remaining authors have nothing to disclose.

Funding

HHS |NIH| National Institute of Diabetes and Digestive and Kidney Diseases (NIDDK), 1RO1DK091623-06; HHS |NIH| National Institute of Diabetes and Digestive and Kidney Diseases (NIDDK): P30DK079312-13.

Author Contributions

Conceptualization: Bruce A. Molitoris, Mark C. Wagner.
Formal analysis: Silvia B. Campos, Carrie L. Phillips, Ruben M. Sandoval.
Funding acquisition: Bruce A. Molitoris.
Investigation: Ruben M. Sandoval, Mark C. Wagner, Shiv Pratap S. Yadav.
Methodology: Silvia B. Campos, Bruce A. Molitoris, George J. Rhodes, Ruben M. Sandoval, Mark C. Wagner, Shiv Pratap S. Yadav.
Project administration: Bruce A. Molitoris.
Resources: Bruce A. Molitoris.
Supervision: Bruce A. Molitoris, Carrie L. Phillips.
Validation: Bruce A. Molitoris, Carrie L. Phillips.
Writing – original draft: Bruce A. Molitoris, Ruben M. Sandoval, Mark C. Wagner.
Writing – review & editing: Bruce A. Molitoris, Ruben M. Sandoval, Mark C. Wagner.

Data Sharing Statement

All data are included in the manuscript and/or supporting information.

Supplemental Material

This article contains the following supplemental material online at http://links.lww.com/KN9/A330.
Supplemental Figure 1.
Supplemental Table 1.

References

1. Perazella MA. Pharmacology behind common drug nephrotoxicities. *Clin J Am Soc Nephrol*. 2018;13(12):1897–1908. doi:10.2215/CJN.00150118
2. Molitoris BA, Sandoval RM, Yadav SPS, Wagner MC. Albumin uptake and processing by the proximal tubule: physiologic, pathologic and therapeutic implications. *Physiol Rev*. 2022;102(4):1625–1667. doi:10.1152/physrev.00014.2021
3. Liu X-F, Wei J, Zhou Q, et al. Immunotoxin SS1P is rapidly removed by proximal tubule cells of kidney, whose damage contributes to albumin loss in urine. *Proc Natl Acad Sci U S A*. 2020;117(11):6086–6091. doi:10.1073/pnas.1919038117
4. Doherty GJ, McMahon HT. Mechanisms of endocytosis. *Annu Rev Biochem*. 2009;78(1):857–902. doi:10.1146/annurev.biochem.78.081307.110540
5. Eshbach ML, Weisz OA. Receptor-mediated endocytosis in the proximal tubule. *Annu Rev Physiol*. 2017;79(1):425–448. doi:10.1146/annurev-physiol-022516-034234
6. Mayor S, Parton RG, Donaldson JG. Clathrin-independent pathways of endocytosis. *Cold Spring Harb Perspect Biol*. 2014;6(6):a016758. doi:10.1101/cshperspect.a016758
7. Renard H-F, Boucrot E. Unconventional endocytic mechanisms. *Curr Opin Cell Biol*. 2021;71:120–129. doi:10.1016/j.ceb.2021.03.001
8. Schuh CD, Polesel M, Platonova E, et al. Combined structural and functional imaging of the kidney reveals major axial differences

in proximal tubule endocytosis. *J Am Soc Nephrol.* 2018;29(11):2696–2712. doi:10.1681/ASN.2018050522
9. Herz J, Goldstein JL, Strickland DK, Ho YK, Brown MS. 39-kDa protein modulates binding of ligands to low density lipoprotein receptor-related protein/alpha 2-macroglobulin receptor. *J Biol Chem.* 1991;266(31):21232–21238. doi:10.1016/s0021-9258(18)54845-6
10. Willnow TE, Rohlmann A, Horton J, et al. RAP, a specialized chaperone, prevents ligand-induced ER retention and degradation of LDL receptor-related endocytic receptors. *EMBO J.* 1996;15(11):2632–2639. doi:10.1002/j.1460-2075.1996.tb00623.x
11. Sengul S, Erturk S, Khan AM, Batuman V, Bradwell A. Receptor-associated protein blocks internalization and cytotoxicity of myeloma light chain in cultured human proximal tubular cells. *PLoS One.* 2013;8(7):e70276. doi:10.1371/journal.pone.0070276
12. Smith CP, Lee W-K, Haley M, Poulsen SB, Thévenod F, Fenton RA. Proximal tubule transferrin uptake is modulated by cellular iron and mediated by apical membrane megalin-cubilin complex and transferrin receptor 1. *J Biol Chem.* 2019;294(17):7025–7036. doi:10.1074/jbc.ra118.006390
13. Zhai XY, Nielsen R, Birn H, et al. Cubilin- and megalin-mediated uptake of albumin in cultured proximal tubule cells of opossum kidney. *Kidney Int.* 2000;58(4):1523–1533. doi:10.1046/j.1523-1755.2000.00314.x
14. Cui S, Verroust PJ, Moestrup SK, Christensen EI. Megalin/gp330 mediates uptake of albumin in renal proximal tubule. *Am J Physiol.* 1996;271(4):F900–F907. doi:10.1152/ajprenal.1996.271.4.f900
15. Prasad JM, Migliorini M, Galisteo R, Strickland DK. Generation of a potent low density lipoprotein receptor-related protein 1 (LRP1) antagonist by engineering a stable form of the receptor-associated protein (RAP) D3 domain. *J Biol Chem.* 2015;290(28):17262–17268. doi:10.1074/jbc.M115.660084
16. Yadav SPS, Sandoval R, Zhao J, et al. Mechanism of how carbamylation reduces albumin binding to FcRn contributing to increased vascular clearance. *Am J Physiol Renal Physiol.* 2021;320(1):F114–F129. doi:10.1152/ajprenal.00428.2020
17. Wagner MC, Myslinski J, Pratap S, et al. Mechanism of increased clearance of glycated albumin by proximal tubule cells. *Am J Physiol Renal Physiol.* 2016;310(10):F1089–F1102. doi:10.1152/ajprenal.00605.2015
18. Sandoval RM, Wagner MC, Patel M, et al. Multiple factors influence glomerular albumin permeability in rats. *J Am Soc Nephrol.* 2012;23(3):447–457. doi:10.1681/ASN.2011070666
19. Zhuo JL, Li XC. Proximal nephron. *Compr Physiol.* 2013;3(3):1079–1123. doi:10.1002/cphy.c110061
20. Molitoris BA, Sandoval RM, Wagner MC. Intravital multiphoton microscopy as a tool for studying renal physiology, pathophysiology and therapeutics. *Front Physiol.* 2022;13:827280. doi:10.3389/fphys.2022.827280
21. Sandoval RM, Molitoris BA. Quantifying endocytosis in vivo using intravital two-photon microscopy. *Methods Mol Biol.* 2008;440:389–402. doi:10.1007/978-1-59745-178-9_28
22. Sundin DP, Meyer C, Dahl R, Geerdes A, Sandoval R, Molitoris BA. Cellular mechanism of aminoglycoside tolerance in long-term gentamicin treatment. *Am J Physiol.* 1997;272(4):C1309–C1318, doi:10.1152/ajpcell.1997.272.4.c1309
23. Sundin DP, Sandoval R, Molitoris BA. Gentamicin inhibits renal protein and phospholipid metabolism in rats: implications involving intracellular trafficking. *J Am Soc Nephrol.* 2001;12(1):114–123. doi:10.1681/ASN.v121114
24. Rosin DL, Hall JP, Zheng S, et al. Human recombinant alkaline phosphatase (ilofotase alfa) protects against kidney ischemia-reperfusion injury in mice and rats through adenosine receptors. *Front Med (Lausanne).* 2022;9:931293. doi:10.3389/fmed.2022.931293
25. Wagner MC, Campos-Bilderback SB, Chowdhury M, et al.. Proximal tubules have the capacity to regulate uptake of albumin. *J Am Soc Nephrol.* 2016;27(2):482–494. doi:10.1681/ASN.2014111107
26. Sandoval RM, Molitoris BA. Intravital multiphoton microscopy as a tool for studying renal physiology and pathophysiology. *Methods.* 2017;128:20–32. doi:10.1016/j.ymeth.2017.07.014
27. Sandoval RM, Molitoris BA, Palygin O. Fluorescent imaging and microscopy for dynamic processes in rats. *Methods Mol Biol.* 2019;208:151–175. doi:10.1007/978-1-4939-9581-3_7
28. Atthe BK, Babsky AM, Hopewell PN, Phillips CL, Molitoris BA, Bansal N. Early monitoring of acute tubular necrosis in the rat kidney by 23Na-MRI. *Am J Physiol Renal Physiol.* 2009;297(5):F1288–F1298. doi:10.1152/ajprenal.00388.2009
29. Sandoval RM, Reilly JP, Running W, et al. A non-nephrotoxic gentamicin congener that retains antimicrobial efficacy. *J Am Soc Nephrol.* 2006;17(10):2697–2705. doi:10.1681/ASN.2005101124
30. Jablonski P, Howden BO, Rae DA, Birrell CS, Marshall VC, Tange J. An experimental model for assessment of renal recovery from warm ischemia. *Transplantation.* 1983;35(3):198–204. doi:10.1097/00007890-198303000-00002
31. Kelly KJ, Tolkoff-Rubin NE, Rubin RH, et al. An oral platelet-activating factor antagonist, Ro-24-4736, protects the rat kidney from ischémie injury. *Am J Physiol.* 1996;271:F1061–F1067. doi:10.1152/ajprenal.1996.271.5.F1061
32. Polesel M, Kaminska M, Haenni D, et al. Spatiotemporal organisation of protein processing in the kidney. *Nat Commun.* 2022;13(1):5732. doi:10.1038/s41467-022-33469-5
33. Dagil R, O'Shea C, Nykjær A, Bonvin AMJJ, Kragelund BB. Gentamicin binds to the megalin receptor as a competitive inhibitor using the common ligand binding motif of complement type repeats: insight from the nmr structure of the 10th complement type repeat domain alone and in complex with gentamicin. *J Biol Chem.* 2013;288(6):4424–4435. doi:10.1074/jbc.m112.434159
34. Humes HD, Sastrasinh M, Weinberg JM. Calcium is a competitive inhibitor of gentamicin-renal membrane binding interactions and dietary calcium supplementation protects against gentamicin nephrotoxicity. *J Clin Invest.* 1984;73(1):134–147. doi:10.1172/jci111184
35. Lesniak W, Pecoraro VL, Schacht J. Ternary complexes of gentamicin with iron and lipid catalyze formation of reactive oxygen species. *Chem Res Toxicol.* 2005;18(2):357–364. doi:10.1021/tx0496946
36. Morán-Zendejas R, Delgado-Ramírez M, Xu J, et al. In vitro and in silico characterization of the inhibition of Kir4.1 channels by aminoglycoside antibiotics. *Br J Pharmacol.* 2020;177(19):4548–4560. doi:10.1111/bph.15214
37. Lin L, Wagner MC, Cocklin R, et al. The antibiotic gentamicin inhibits specific protein trafficking functions of the Arf1/2 family of GTPases. *Antimicrob Agents Chemother.* 2011;55(1):246–254. doi:10.1128/aac.00450-10
38. Molitoris BA. Cell biology of aminoglycoside nephrotoxicity: newer aspects. *Curr Opin Nephrol Hypertens.* 1997;6(4):384–388. doi:10.1097/00041552-199707000-00013
39. Sandoval RM, Dunn KW, Molitoris BA. Gentamicin traffics rapidly and directly to the Golgi complex in LLC-PK1 cells. *Am J Physiol Renal Physiol.* 2000;279(5):F884–F890. doi:10.1152/ajprenal.2000.279.5.f884
40. Hall AM, Rhodes GJ, Sandoval RM, Corridon PR, Molitoris BA. In vivo multiphoton imaging of mitochondrial structure and function during acute kidney injury. *Kidney Int.* 2013;83(1):72–83. doi:10.1038/ki.2012.328
41. Sandoval RM, Molitoris BA. Gentamicin traffics retrograde through the secretory pathway and is released in the cytosol via the endoplasmic reticulum. *Am J Physiol Renal Physiol.* 2004;286(4):F617–F624. doi:10.1152/ajprenal.00130.2003
42. Sandvig K, Kavaliauskiene S, Skotland T. The protein toxins ricin and shiga toxin as tools to explore cellular mechanisms of internalization and intracellular transport. *Toxins (Basel).* 2021;13(6):377. doi:10.3390/toxins13060377
43. Tenten V, Menzel S, Kunter U, et al. Albumin is recycled from the primary urine by tubular transcytosis. *J Am Soc Nephrol.* 2013;24(12):1966–1980. doi:10.1681/ASN.2013010018
44. Hori Y, Aoki N, Kuwahara S, et al. Megalin blockade with cilastatin suppresses drug-induced nephrotoxicity. *J Am Soc Nephrol.* 2017;28(6):1783–1791. doi:10.1681/ASN.2016060606
45. Shayan M, Elyasi S. Cilastatin as a protective agent against drug-induced nephrotoxicity: a literature review. *Expert Opin Drug Saf.* 2020;19(8):999–1010. doi:10.1080/14740338.2020.1796967

46. Dunn KW, Molitoris BA, Dagher PC. The Indiana O'brien center for advanced renal microscopic analysis. *Am J Physiol Renal Physiol.* 2021;320(5):F671–F682. doi:10.1152/ajprenal.00007.2021
47. Onodera A, Tani M, Michigami T, et al. Role of megalin and the soluble form of its ligand RAP in Cd-metallothionein endocytosis and Cd-metallothionein-induced nephrotoxicity in vivo. *Toxicol Lett.* 2012;212(2): 91–96. doi: 10.1016/j.toxlet.2012.05.012
48. Kristiansen M, Kozyraki R, Jacobsen C, et al. Molecular dissection of the intrinsic factor-vitamin B12 receptor, cubilin, discloses regions important for membrane association and ligand binding. *J Biol Chem.* 1999;274(29):20540–20544. doi:10.1016/j.toxlet.2012.05.012
49. Orlando Ra, Exner M, Czekay RP, et al. Identification of the second cluster of ligand-binding repeats in megalin as a site for receptor-ligand interactions. *Proc Natl Acad Sci U S A.* 1997; 94(6):2368–2373. doi:10.1073/pnas.94.6.2368
50. Polesel M, Hall AM. Axial differences in endocytosis along the kidney proximal tubule. *Am J Physiol Renal Physiol.* 2019;317(6): F1526–F1530. doi:10.1152/ajprenal.00459.2019

Received: June 21, 2022 **Accepted:** January 31, 2023
Published Online Ahead of Print: February 27, 2023

See related editorial, "Endocytosis and Nephrotoxicity—It's a RAP!," on pages 572–574.